included goat antibody to rat CD4, CD8, and F480; hamster antibody to mouse TCRαβ and TCRγδ (PharMingen); rat antibody to mouse β_7 integrin (PharMingen); sheep antibody to mouse IgA (Sigma); donkey antibody to mouse IgG (Jackson ImmunoResearch); rat antibody to MHC class II (OX-3; Serotec); and rabbit antibody to β-catenin (*2*).
12. M. L. Hermiston and J. I. Gordon, unpublished observations.
13. R. H. Riddell, in *Inflammatory Bowel Disease*, J. B. Kirsner and R. G. Shorter, Eds. (Williams & Wilkins, Baltimore, ed. 4, 1995), pp. 517–552.
14. D. K. Podolsky, *N. Engl. J. Med.* **325**, 928 (1991).
15. P. Mombaerts *et al.*, *Cell* **75**, 275 (1993); B. Sadlack *et al.*, *ibid.*, p. 253; R. Kühn *et al.*, *ibid.*, p. 263.
16. W. Birchmeier and J. Behrens, *Biochim. Biophys. Acta* **1198**, 11 (1994).
17. L.-K. Su *et al.*, *Science* **256**, 668 (1992); A. R. Moser, W. F. Dove *et al.*, *J. Cell Biol.* **116**, 1517 (1992).
18. B. Rubinfeld *et al.*, *Science* **262**, 1731 (1993); L.-K. Su *et al.*, *ibid.*, p. 1734; B. Rubinfeld *et al.*, *J. Biol. Chem.* **270**, 5549 (1995).
19. B. Levin, in (*13*), pp. 461–473.
20. H. Komano *et al.*, *Proc. Natl. Acad. Sci. U.S.A.* **92**, 6147 (1995).
21. K. L. Cepek *et al.*, *Nature* **372**, 190 (1994).
22. N. A. Wright, C. Pike, G. Eli, *ibid.* **343**, 82 (1990); D. J. Ahnen *et al.*, *J. Pathol.* **173**, 317 (1994).
23. We thank D. O'Donnell for technical assistance, P. Swanson for reviewing the histopathology, E. Unanue for goat antibody to rat CD4, CD8, and F480, W. J. Nelson for antibody to β-catenin, and C. Kintner for pSP72NCADΔC. Supported in part by NIH grants DK39760 and DK30292.

11 July 1995; accepted 20 September 1995

Concerted Signaling by Retinal Ganglion Cells

Markus Meister,* Leon Lagnado,† Denis A. Baylor

To analyze the rules that govern communication between eye and brain, visual responses were recorded from an intact salamander retina. Parallel observation of many retinal ganglion cells with a microelectrode array showed that nearby neurons often fired synchronously, with spike delays of less than 10 milliseconds. The frequency of such synchronous spikes exceeded the correlation expected from a shared visual stimulus up to 20-fold. Synchronous firing persisted under a variety of visual stimuli and accounted for the majority of action potentials recorded. Analysis of receptive fields showed that concerted spikes encoded information not carried by individual cells; they may represent symbols in a multineuronal code for vision.

Current understanding of how the retina transmits the visual scene to the brain is based primarily on electrical recordings from single neurons. As a consequence, the spike trains from different optic nerve fibers have commonly been treated as independent messages about the environment. However, pairwise recordings from retinal ganglion cells in goldfish (*1*), rabbits (*2*), and cats (*3–5*) have shown that this assumption is violated—nearby cells of similar functional type have a strong tendency to fire synchronously. These measurements were all obtained in darkness or under constant uniform illumination [but see (*6*)], when ganglion cells fire sporadically, and thus it was not possible to assess the function of such correlations in visual signaling. It has been suggested that synchronous firing during visual stimulation would imply redundancy among neuronal messages and thus an inefficient use of the optic nerve (*2*).

To assess the importance of concerted firing in visual signaling, we used a microelectrode array to record simultaneously the spike trains of 30 to 50 ganglion cells in an isolated salamander retina (*7*). This preparation contains large hardy neurons and has been used extensively to study the cellular mechanisms of retinal processing. Figure 1A illustrates the responses of two nearby neurons to spatially uniform illumination that regularly switched between two intensity levels. Although each cell fired only a few spikes per stimulus period, at times that varied by several hundred milliseconds from trial to trial, the spikes from the two cells appeared to be tightly locked to each other in time. The mean firing rate of each neuron was strongly modulated by the periodic stimulus (Fig. 1B), and as a result, the correlation function between the two spike trains showed a pronounced periodic component (Fig. 1C). However, this stimulus-induced correlation was dwarfed by a tall peak near zero delay, with a full width at half maximum of only 20 ms (Fig. 1D). This strong tendency to fire in near-synchrony shows that the two neurons did not respond to light independently.

To quantify the strength of concerted firing, action potentials from cells 1 and 2 were defined as a spike pair if they occurred within 20 ms of each other. We then computed a correlation index as the number of spike pairs observed divided by the number expected if the two neurons responded independently (*8*). For the cell pair in Fig. 1, this index was 12.4, so that tightly linked pairs of spikes occurred about 12 times more frequently than was expected. Such anomalous pairing accounted for 60% of all spikes generated by cell 1 and 42% of spikes generated by cell 2. We computed correlation functions for all pairs among 32 cells in this retina: 31% of the pairs showed clear evidence of concerted firing, with a correlation peak near zero delay whose shape was similar to that shown in Fig. 1D, though it varied in amplitude. Further statistical analysis revealed that synchronous firing events generally extended over more than two neurons (*9*). Overall, these patterns of concerted firing accounted for approximately 50% of all action potentials from the recorded sample of ganglion cells. Because the electrode array typically monitored only 10% of the overlying ganglion cells, we probably missed many synchronous firing patterns. Thus, the fractional contribution of concerted firing to the retinal output may well exceed 50%.

The correlation index varied with the distance between the two neurons' receptive fields (Fig. 2). It decreased from a maximum of 20 at short distances by a factor of e over 200 μm. In comparison, the centers of these neurons' receptive fields had approximately Gaussian-shaped profiles (*10*), with an average radius of 120 μm. Concerted firing thus appears to be associated with overlap of receptive-field centers. At distances between 400 and 1000 μm, the correlation index dropped significantly below 1, indicating that more distant cells avoided firing together. When separated by more than 1000 μm, ganglion cells appeared to signal independently as assessed by this test. When the ganglion cells were sorted by functional type (*10*), it was found that pairs of "fast OFF" cells (Fig. 2A) exhibited more synchronous firing than did pairs of "slow OFF" cells (Fig. 2B), whereas pairs of ON cells produced the weakest correlation index (Fig. 2C). ON and OFF cells generally fired independently of each other, although some pairs with strong correlations were found at short distances (Fig. 2D). The shape of the correlation function (Fig. 1D) and its dependence on overlap of receptive fields (Fig. 2), as well as the dominance of synchronous firing among neurons with transient responses (Fig. 2A), are remarkably similar to the observations of Mastronarde (*3*) on cat ganglion cells under uniform illumination. In contrast to that study, we generally did not observe a sharp well in the cross-correlogram between an ON cell and an OFF cell. Furthermore, the negative correlation among cells of the same class at distances greater than 400 μm has not been reported previously.

M. Meister, Department of Molecular and Cellular Biology, Harvard University, 16 Divinity Avenue, Cambridge, MA 02138, USA. E-mail: meister@biosun.harvard.edu
L. Lagnado and D. A. Baylor, Department of Neurobiology, Sherman Fairchild Science Building, Stanford University School of Medicine, Stanford, CA 94305-5401, USA.

*To whom correspondence should be addressed.
†Present address: Medical Research Council Laboratory of Molecular Biology, Hills Road, Cambridge CB22QH, UK.

Apparently, synchronous firing is a major component of retinal activity even during visual stimulation. The role of these correlations in retinal signaling depends on whether synchronous spike pairs are driven by the stimulus or by a noise source outside the visual pathway. To examine this, we measured the receptive fields of spike pairs by reverse correlation to a pseudorandom flickering checkerboard (*11*, *12*). In all cases, the spike pair was visually driven. Its sensitivity profile was generally smaller than that of the two parent cells and was located in the region of overlap between the two parent receptive fields (Fig. 3). If the two neurons operated independently, the spike pair's reverse correlation should approximate the sum of the two parent profiles, rather than their intersection (*13*). Thus, spike pairs encoded information not contained in the individual spike trains of the two parent ganglion cells.

Two ganglion cells with overlapping receptive-field centers share input from a common group of photoreceptors. In some species, stochastic fluctuations within the photoreceptors seem to account for the variation in the retinal response (*14*), and such noise has also been proposed as the source of correlations among ganglion cells (*2*, *4*). To test whether shared photoreceptor signals can account for the synchronized firing observed here, we deliberately introduced stochastic fluctuations in the receptors by stimulation with a flickering checkerboard. For pairs of ganglion cells with overlapping receptive fields, two types of correlation function were observed. One type was consistent with an origin in shared photoreceptors (Fig. 4A). It showed broad peaks or valleys near zero delay, whose shape depended on the response class of the component cells. Its time course slowed systematically as the mean stimulus intensity was decreased, probably reflecting

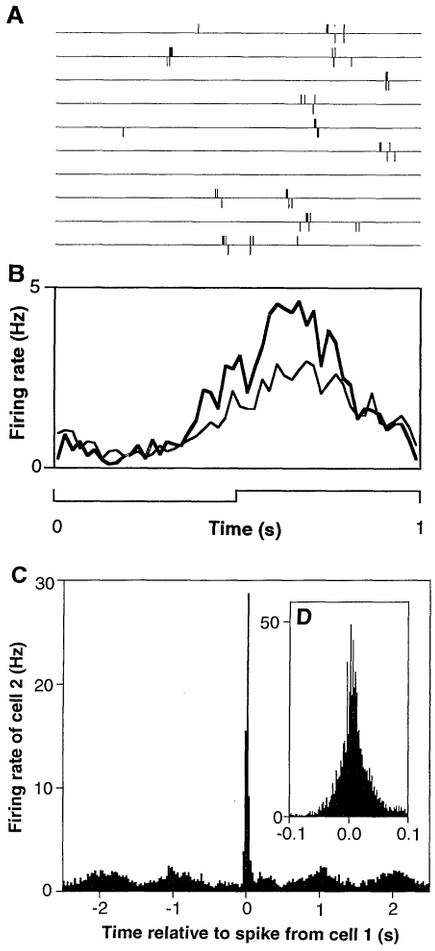

Fig. 1. Responses of two OFF-type ganglion cells to periodic flashes. The stimulus consisted of full-field illumination with white light, square-wave modulated with a period of 1 s between intensities of 9.4×10^{-6} W/m^2 (357 isomerizations/s per rod) and 11.1×10^{-6} W/m^2 (422 isomerizations/s per rod). The recording lasted for 1300 s, yielding 2333 spikes from cell 1 and 1774 spikes from cell 2. (**A**) Firing times of cell 1 (upward ticks) and cell 2 (downward ticks) during 10 successive flashes. (**B**) Average firing rates of cell 1 (thick line) and cell 2 (thin line), computed by histogramming of the spike times relative to the preceding light step in 20-ms bins. (**C**) Cross-correlation function between the two spike trains (*16*), obtained by histogramming of the pairwise differences between spike times of cells 1 and 2 in 25-ms bins. (**D**) The central peak of (C) on an expanded time scale with 2-ms bins.

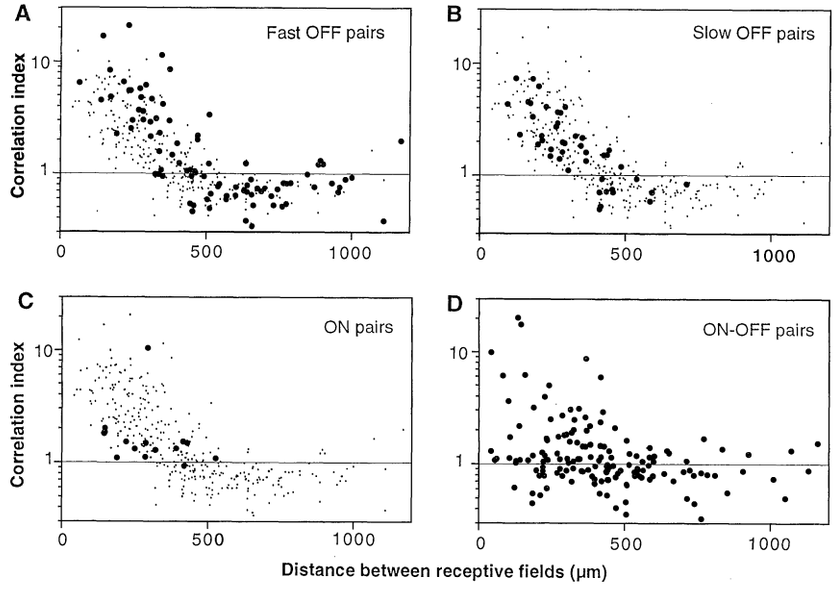

Fig. 2. The correlation index for each pair of cells among 32 neurons, as a function of the distance between the centers of their receptive fields, determined under periodic flash stimulation as in Fig. 1. Each cell was classified according to its visual response properties (*10*). Large dots identify pairs of fast OFF cells (**A**), slow OFF cells (**B**), ON cells (**C**), and pairs composed of an ON and an OFF cell (**D**). For comparison, the small dots in (A), (B), and (C) identify all ON-ON and OFF-OFF pairs.

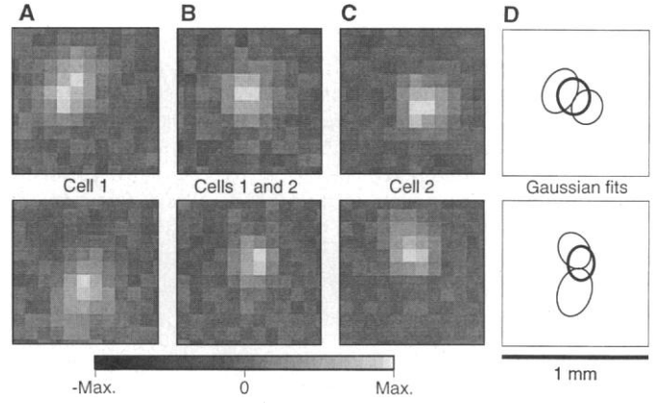

Fig. 3. The receptive-field profiles of two individual cells (**A** and **C**) and their synchronous spike pairs (**B**), determined by reverse correlation to a flickering checkerboard stimulus [pixel size 90 μm, flicker interval 120 ms, and mean intensity 1.69×10^{-4} W/m^2 (see *12*)]. White corresponds to the maximal sensitivity in the center of the receptive field, 50% gray corresponds to zero sensitivity, and darker grays correspond to sensitivities antagonistic to that of the center. (**D**) shows the contours at one standard deviation from the center for Gaussian fits to the profiles in (A) and (C) (thin lines) and in (B) (thick line). The top and bottom rows of plots are from two different cell pairs.

changes in photoreceptor response kinetics during the shift from cones to rods and adaptation within the rods (*15*). In darkness, the correlation function was of similar shape but was less strongly modulated, suggesting that at least part of the dark activity derived from photoreceptor fluctuations similar to those produced by dim flickering light (*4*). However, the correlation function derived from other cell pairs had a single sharp peak near zero. Its shape was independent of the mean light intensity and persisted unaltered in darkness (Fig. 4B), which is inconsistent with an origin in the slow fluctuations of photoreceptors. This class of correlation functions accounted for the high values of the correlation index in Fig. 2, and showed a similar distance dependence at all light levels, including darkness.

To produce the sharp peak in the correlation function (Fig. 1D), the input signal shared by the two observed ganglion cells must consist of very brief events that depolarize the postsynaptic ganglion cells for only 10 to 20 ms. Furthermore, these depolarizations must be strong, reliably triggering action potentials in both ganglion cells, even though each of them also receives input from other unshared sources. By contrast, the shared input can be loosely coupled to the visual stimulus, with trial-to-trial variations in the response time of up to several hundred milliseconds in dim light (Fig. 1A) and spontaneous activity in darkness (Fig. 4B). Given the circuitry of the inner retina, this shared input might be delivered by a bipolar cell, an amacrine cell, or a third ganglion cell (through gap junctions). Bipolar cells produce slow potentials, which are unlikely to trigger precisely synchronous ganglion cell spikes. Action potentials in a third ganglion cell could have the desired effect, but we rarely encountered correlation functions with a dip at zero as would be expected from direct transmission between ganglion cells (*5*, *16*). It appears more likely that the synchronizing input derives from an unobserved spiking neuron, for example, a spiking amacrine cell (*3*, *17*).

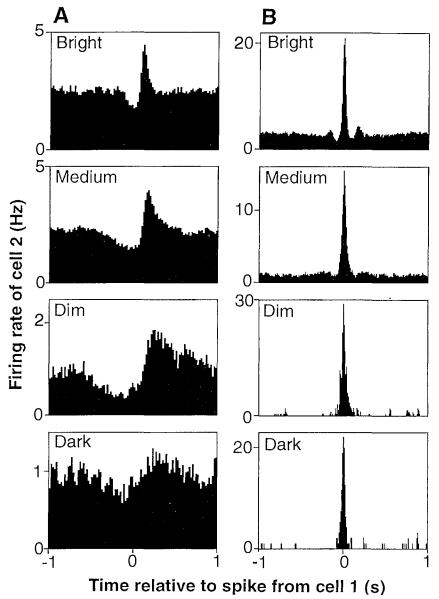

Fig. 4. Correlation function between two ganglion cell spike trains under random flicker stimulation as in Fig. 3, performed at various mean intensities: 2.32×10^{-2} W/m^2 (bright); 2.63×10^{-3} W/m^2 (medium); 1.69×10^{-4} W/m^2 (dim); and in darkness. (**A**) An ON and an OFF cell separated by 140 μm. (**B**) Two OFF cells separated by 130 μm.

It has been proposed that the primary task of the retina is to reduce redundancy in the messages that encode visual scenes. Redundancy results because nearby points in a natural image are likely to have similar intensities (*18*), because the local intensity tends to vary slowly, and because the absorption spectra of different photoreceptor pigments overlap substantially. In this view, lateral inhibition, temporal adaptation, and spectral antagonism all act to produce a more de-correlated and compact representation of the visual scene at the level of the optic nerve (*19*). At first sight, the finding of strong correlations among retinal ganglion cells appears to contradict this hypothesis and suggests an inefficient use of the optic nerve, with many nerve fibers carrying the same signal. On the other hand, any given ganglion cell can participate in several groups of synchronously firing cells. Thus, the retina might use a combinatorial code for vision, whose elementary symbols are multineuronal firing patterns rather than single action potentials from individual cells. The analysis in Fig. 3 provides some support for this proposal, because the spatial receptive field of a spike pair was different from that of the component single neurons and was often more sharply defined in space. Presumably, this reflects the receptive field of the interneuron that delivered the shared excitation to ganglion cells. Vice versa, each characteristic group of synchronous spikes among ganglion cells signals the firing of the corresponding interneuron. Thus, spikes from interneurons, such as amacrine cells, could be multiplexed into the retinal output without adding more fibers to the optic nerve (*20*).

It appears that retinal ganglion cells should not be considered independent channels of information about the visual environment. The present work shows that a sizable proportion of ganglion cell activity violates this assumption and earlier paired recordings suggest that this finding holds true in a variety of species. These patterns of concerted firing must be considered when one interprets the function of visual centers in the brain. In particular, if concerted firings form the symbols of a distributed neural code, one expects to find neural circuitry that detects such activity in optic nerve fibers.

REFERENCES AND NOTES

1. D. W. Arnett, *Exp. Brain Res.* **32**, 49 (1978); J. A. Johnsen and M. W. Levine, *J. Physiol.* **345**, 439 (1983).
2. D. Arnett and T. E. Spraker, *J. Physiol.* **317**, 29 (1981).
3. D. N. Mastronarde, *J. Neurophysiol.* **49**, 303 (1983).
4. ———, *ibid.*, p. 325.
5. ———, *ibid.*, p. 350.
6. K. S. Ginsburg, J. A. Johnsen, M. W. Levine, *J. Physiol.* **351**, 433 (1984).
7. The retina of a larval tiger salamander was isolated into Ringer's medium, and action potentials were recorded from the ganglion cells with an extracellular electrode array; stimuli were delivered by a computer monitor and projected onto the photoreceptor layer, as described previously (*12*). We have observed the basic phenomenon of distance-dependent synchronous firing in each of 13 salamander retinas analyzed to date; the detailed results presented here are based on a total of 122 ganglion cells and 2446 cell pairs from 3 retinas.
8. We found the rate at which synchronous spike pairs occurred by integrating the correlation function (Fig. 1C) under the central peak from −0.020 s to 0.020 s. We estimated the rate expected from independent processing by integrating over the corresponding interval one stimulus period removed from zero delay (0.980 to 1.020 s), a test known as "shift prediction" (*16*). The correlation index is the ratio of observed rate to expected rate. Its expectation value is 1 if the two neurons respond to light independently of each other.
9. To identify statistically significant patterns of synchronous firing that extend across many neurons, one first determines which two among the n cells in the data set are most strongly correlated by synchronous firing (within ±20 ms); all such spike pairs from these cells are recoded by a spike in a newly defined $(n + 1)^{st}$ spike train and removed from the two original spike trains. Then one iterates the same pairwise correlation analysis, adding a newly defined event train each time, until no significant spike pairs remain. With this algorithm, synchronous firing patterns involving up to six neurons were detected in a simultaneous recording from 44 cells (M. Schnitzer and M. Meister, in preparation).
10. We determined spatio-temporal receptive fields by stimulating the retina with a pseudorandom flickering checkerboard and then reverse-correlating each ganglion cell's response with the stimulus (M. Meister, in preparation) (*12*). Functional types of salamander ganglion cells were distinguished by the time course of their reverse correlation. When exposed to a diffuse flash of light, the ON cells produce a transient response at light onset, the fast OFF cells show a rapid transient response to light offset, and slow OFF cells respond transiently with longer latency and can produce ON-OFF responses to flashes of sufficiently high contrast. The spatial profile of each receptive field was fitted with a two-dimensional Gaussian surface to estimate the location of the field center.
11. G. M. Ghose, I. Ohzawa, R. D. Freeman, *J. Neurophysiol.* **71**, 330 (1994).
12. M. Meister, J. Pine, D. A. Baylor, *J. Neurosci. Methods* **51**, 95 (1994).
13. This can be seen as follows: First consider two ganglion cells with nonoverlapping receptive fields, driven by a randomly flickering checkerboard. For a synchronous spike pair to occur, both cells must be excited simultaneously. Thus, the reverse correlation of the spike pair—which is equal to the mean stimulus preceding such an event—will include both receptive-field profiles. As the two receptive fields approach each other, this relation is maintained, and the reverse correlation of the spike pair approximates the sum of the two single-cell reverse correlations. If, instead of random flicker, a single small spot were used to probe responses, the receptive

field for joint spikes should approximate the intersection of the two single-cell fields.
14. H. B. Barlow, W. R. Levick, M. Yoon, *Vision Res. Suppl.* **3**, 87 (1971); A.-C. Aho, K. Donner, C. Hydén, L. O. Larsen, T. Reuter, *Nature* **334**, 348 (1988); D. A. Baylor, G. Matthews, K. W. Yau, *J. Physiol.* **309**, 591 (1980).
15. D. A. Baylor, T. D. Lamb, K. W. Yau, *J. Physiol.* **288**, 589 (1979).
16. G. P. Moore, J. P. Segundo, D. H. Perkel, H. Levitan, *Biophys. J.* **10**, 876 (1970).
17. Amacrine cells in salamander retina have been associated with inhibitory effects [F. Werblin, G. Maguire, P. Lukasiewicz, S. Eliasof, S. M. Wu, *Visual Neurosci.* **1**, 317 (1988); D. F. Wunk and F. S. Werblin, *J. Gen. Physiol.* **73**, 265 (1979)], but this diverse cell class may well contain excitatory neurons, as is true of other species [T. Millar *et al.*, *Neurosci. Lett.* **61**, 311 (1985); R. H. Masland, J. W. Mills, C. Cassidy, *Proc. R. Soc. London B* **223**, 121 (1984); R. D. Glickman, A. R. Adolph, J. E. Dowling, *Brain Res.* **234**, 81 (1982); G. D. Guiloff and H. Kolb, *Vision Res.* **32**, 2023 (1992)]. Excitatory transmission between amacrine and ganglion cells has been observed directly in catfish [H. M. Sakai and K. I. Naka, *J. Neurophysiol.* **63**, 105 (1990)] and may be mediated by the gap junctions that link many neurons in the inner retina [D. I. Vaney, *Progr. Retinal Eye Res.* **13**, 301 (1994)] OFF bipolar cells display occasional fast depolarizing transients [B. R. Maple, F. S. Werblin, S. M. Wu, *Vision Res.* **34**, 2357 (1994)] that might also be large enough to synchronize two ganglion cells.
18. D. J. Field, *J. Opt. Soc. Am.* **4**, 2379 (1987).
19. H. B. Barlow, in *Sensory Communication*, W. A. Rosenblith, Ed. (MIT Press, Cambridge, MA, 1961), pp. 217–234; G. Buchsbaum and A. Gottschalk, *Proc. R. Soc. London B* **220**, 89 (1983); J. J. Atick, *Network* **3**, 213 (1992).
20. This is possible because the bandwidth of the visual signal, after transduction by the photoreceptors, is on the order of a few hertz, whereas the bandwidth of optic nerve fibers extends to 100 Hz; the difference between the bandwidths of the signal and carrier is available for multiplexing. A more detailed analysis shows that this can greatly enhance information transmission through the optic nerve as compared with a single-neuron code (M. Meister, *Proc. Natl. Acad. Sci. U.S.A.*, in press).
21. We thank R. Schneeveis for expert technical assistance. Supported by a Lucille P. Markey Scholarship and National Eye Institute (NEI) grant EY10020 to M.M., by a fellowship from the Human Frontiers in Science Project to L.L., and by NEI grants EY01543 and EY05750 to D.A.B.

28 June 1995; accepted 13 September 1995

Pheromone Response in Yeast: Association of Bem1p with Proteins of the MAP Kinase Cascade and Actin

Thomas Leeuw, Anne Fourest-Lieuvin, Cunle Wu, Janet Chenevert,* Karen Clark,† Malcolm Whiteway, David Y. Thomas, Ekkehard Leberer‡

Haploid cells of the yeast *Saccharomyces cerevisiae* respond to mating pheromones with polarized growth toward the mating partner. This morphological response requires the function of the cell polarity establishment protein Bem1p. Immunochemical and two-hybrid protein interaction assays revealed that Bem1p interacts with two components of the pheromone-responsive mitogen-activated protein (MAP) kinase cascade, Ste20p and Ste5p, as well as with actin. Mutants of Bem1p that are associated with defective pheromone-induced polarized morphogenesis interacted with Ste5p and actin but not with Ste20p. Thus, the association of Bem1p with Ste20p and Ste5p may contribute to the conveyance of spatial information that regulates polarized rearrangement of the actin cytoskeleton during yeast mating.

Haploid cells of *S. cerevisiae* secrete the peptide pheromones **a** and α factors to induce the conjugation of cells with opposite mating types. The pheromones bind to specific receptors and thereby trigger differentiation processes (*1*). The responding cells adopt a polarized cell shape with membrane projections directed toward the pheromone source (*2*). Polarized morphogenesis in the direction of an external signal is a characteristic feature of differentiated cells. Examples include chemotactic responses in neutrophils and *Dictyostelium*, polarized growth of T cells toward antigen-presenting cells, and the development of cell polarity during differentiation of epithelial and neuronal cells (*3*). The molecular mechanisms by which the positional information of an external signal is translated into the establishment of cell polarity are poorly understood.

In conjugating yeast cells, development of cell polarity requires the small Rho-like guanosine triphosphate (GTP)–binding protein Cdc42p and its guanosine diphosphate (GDP)–GTP exchange factor Cdc24p, as well as the Src homology 3 (SH3) domain–containing protein Bem1p that associates with Cdc24p (*4*–*6*). These proteins also participate in regulation of the development of cell polarity during budding; this process is under the control of an internal program that includes the function of bud-site selection proteins, which specify the site of bud formation (*7*, *8*). During mating, this internal program must be overridden by spatial information imposed by the external pheromone signal in order to specify the site of cell growth.

The binding of pheromones to their receptors activates a heterotrimeric GTP-binding protein (G protein) common to both cell types. Through the action of the Ste20p protein kinase, the G protein β and γ subunits stimulate a MAP kinase cascade whose components constitute a signaling complex by association with the scaffold protein Ste5p (*9*). Ste20p phosphorylates Ste11p, a MEK (MAP or extracellular signal–regulated kinase kinase) kinase homolog, in vitro (*10*) and is therefore likely to be a constituent of this signaling complex. The *STE20* and *BEM1* genes can function as high-dosage suppressors of a G protein β subunit mutant that is partially defective in signaling (*11*, *12*).

Specific antibodies to Ste20p, Bem1p, Ste5p, and actin (Fig. 1A) were used to investigate the relative distribution of these proteins in yeast cell fractions (*13*). About 50% of total Ste20p and >60% of total Bem1p sedimented with the particulate fraction, which also contained Ste5p and actin (55 and 65%, respectively, of total protein) (*14*). Washing the particulate fraction with increasing concentrations of NaCl solubilized increasing amounts of Ste20p, Bem1p, actin, and, to a lesser extent, Ste5p (Fig. 1B). These proteins were completely solubilized with 1% SDS but remained in the particulate fraction after treatment with NP-40 or Triton X-100 at concentrations that are known to release membrane-bound proteins. The results suggest that Ste20p, Bem1p, and Ste5p are not directly bound to membranes but rather are associated with complexes of high density. Sucrose density gradient centrifugation resolved these complexes into two fractions: a heavy fraction migrating at 46 to 48% (w/w) sucrose that contained actin, and a light fraction migrating at 38 to 40% sucrose that did not contain actin (Fig. 1C). Marker enzymes for Golgi vesicles and the plasma membrane—guanosine diphosphatase (GDPase) and adenosine triphosphatase (ATPase), respectively—did not colocalize precisely with these fractions. These observations are consistent with the view that Ste20p, Bem1p, and Ste5p are constituents of a large protein complex that is partly bound to the actin cytoskeleton and is not directly bound to the membrane.

We next investigated whether Ste20p, Ste5p, and Bem1p are associated in vivo.

T. Leeuw, A. Fourest-Lieuvin, C. Wu, K. Clark, M. Whiteway, D. Y. Thomas, E. Leberer, Eukaryotic Genetics Group, Biotechnology Research Institute, National Research Council of Canada, 6100 Royalmount Avenue, Montreal, Quebec H4P 2R2, Canada.
J. Chenevert, Department of Biochemistry and Biophysics, University of California, San Francisco, CA 94143–0448, USA.

*Present address: Station Zoologique, URA 671 Centre National de la Recherche Scientifique, 06230 Villefranche-sur-mer, France.
†Present address: Department of Botany, University of Maryland, College Park, MD 20742–5815, USA.
‡To whom correspondence should be addressed.